

1 Impact of dams and climate change on 2 suspended sediment flux to the Mekong 3 delta 4

5 Gianbattista Bussi^{1,*}, Stephen E. Darby², Paul G. Whitehead^{1,2}, Li Jin³, Simon J. Dadson¹, Hal
6 E. Voepel², Grigorios Vasilopoulos⁴, Christopher R. Hackney⁵, Craig Hutton², Tristan
7 Berchoux⁶, Daniel R. Parsons⁴, Andrew Nicholas⁷

8 1 – School of Geography and the Environment, University of Oxford, South Parks Road, Oxford, OX1 3QY, UK

9 2 – School of Geography and Environmental Sciences, University of Southampton, Avenue Campus, Highfield Road, Southampton SO17
10 1BJ, UK

11 3 – Geology Department, State University of New York College at Cortland, Cortland, NY 13045, US

12 4 – Energy and Environment Institute, University of Hull, Cottingham Road, Hull HU6 7RX, UK

13 5 - School of Geography, Politics and Sociology, Newcastle University, Newcastle upon Tyne, NE1 7RU UK

14 6 - TETIS, CIHEAM-IAMM, Univ Montpellier, AgroParisTech, CNRS, CIRAD, INRAE, Montpellier, France

15 7 – Department of Geography, University of Exeter, Exeter EX4 4RJ, UK

16 * Corresponding author

17

18 **Abstract**

19 The livelihoods of millions of people living in the world’s deltas are deeply interconnected with the
20 sediment dynamics of these deltas. In particular a sustainable supply of fluvial sediments from
21 upstream is critical for ensuring the fertility of delta soils and for promoting sediment deposition that
22 can offset rising sea levels. Yet, in many large river catchments this supply of sediment is being
23 threatened by the planned construction of large dams. In this study, we apply the INCA hydrological
24 and sediment model to the Mekong River catchment in South East Asia. The aim is to assess the impact
25 of several large dams (both existing and planned) on the suspended sediment fluxes of the river. We
26 force the INCA model with a climate model to assess the interplay of changing climate and sediment
27 trapping caused by dam construction. The results show that historical sediment flux declines are
28 mostly caused by dams built in PR China and that sediment trapping will increase in the future due to
29 the construction of new dams in PDR Lao and Cambodia. If all dams that are currently planned for the
30 next two decades are built, they will induce a decline of suspended sediment flux of 50% (47-53% 90%
31 confidence interval (90%CI)) compared to current levels (99 Mt/y at the delta apex), with potentially
32 damaging consequences for local livelihoods and ecosystems.

33 **Keywords**

34 sediment transport, large dams, INCA model, Mekong River, climate change

35

36 1. Introduction

37 The world's deltas are highly productive environments that support dense populations, but their low-
38 lying land means that they are highly exposed to the threat of rising relative sea level (Ericson et al.,
39 2006; Ibáñez et al., 2014; Syvitski, 2008). Indeed, there is a growing concern that accelerated rates of
40 relative sea-level rise (Syvitski et al., 2009; Tessler et al., 2018) are now leading to an existential crisis
41 for many of the world's deltas (Anthony et al., 2015; Day et al., 2016; Kondolf et al., 2018; Tessler et
42 al., 2016, 2015). In deltas, rising relative sea-levels are driven primarily by a combination of eustatic
43 sea-level rise and local ground subsidence, therefore a sustainable supply of fluvial sediment is critical
44 to promote delta-plain sedimentation and hence prevent, or at least delay, deltas being 'drowned'.

45 A growing body of evidence indicates that the supply of fluvial sediment to many of the world's deltas
46 is being disrupted by environmental change. A number of studies (Darby et al., 2016; Li et al., 2018;
47 Walling, 2008; Walling and Fang, 2003) have shown that major declines in sediment loads to the
48 coastal zone have occurred in recent decades, and a recent global projection (Dunn et al., 2019)
49 highlights that this trend is likely to continue in the future. While natural climate variability can have
50 an impact on sediment fluxes, there is broad consensus that both observed and projected reductions
51 in sediment loads are a consequence of a global boom in dam construction for hydropower
52 development (Grill et al., 2019; Vörösmarty et al., 2003; Zarfl et al., 2015). Importantly, the disrupted
53 and fragmented rivers that feed many of the world's largest and most populous deltas (e.g., Ganges-
54 Brahmaputra, Mekong, Nile) are often large and transboundary. In these systems, the major focus of
55 dam construction may be located in nations upstream of the host delta itself, signifying a need to
56 evaluate the system-wide trade-offs between the benefits of damming and the adverse impacts that
57 may be propagated to downstream reaches and their deltas. In addition, these large rivers also face a
58 range of additional stresses (including anthropogenic climate change) that manifest in variable
59 intensities over the wide expanse of each river's catchment. In such circumstances it can be very
60 challenging to attribute changes in the sediment loads reaching large deltas correctly, which can
61 further inhibit effective trans-border cooperation and governance (Best, 2019).

62 One of the world's largest transboundary river systems is the Mekong. Until relatively recently, the
63 Mekong had remained relatively unaffected by damming (Kummu et al., 2010). However, because of
64 its considerable potential for hydropower generation (up to 268,000 GWh/yr; Schmitt et al., 2019),
65 several hydropower dams have been constructed in recent decades. Others are under construction,
66 nearing completion or planned, both on the main stem and on tributaries (Mekong River Commission,
67 2010, 2009). In its natural state the Mekong historically transported a high load of suspended
68 sediments (160 Mt/yr; Milliman & Meade, 1983) and associated nutrients, which together support the
69 productive ecosystems of the lower Mekong floodplains (Chapman and Darby, 2016) and the world's
70 largest freshwater fishery. The Mekong's dams are likely to reduce the sediment supply to the Mekong
71 delta (Kondolf et al., 2014), with potentially damaging consequences on the agriculture, fishery and
72 ecosystem of the delta (Baran and Myschowoda, 2009).

73 With large areas of the Mekong at risk of subsiding below mean sea level by 2100 (Minderhoud et al.,
74 2019), continued fluvial sedimentation is key to offsetting the effects of land subsidence and sea level
75 rise. Therefore, it is important to understand recent and future trends in fluvial suspended sediment
76 flux and attribute changes to the correct cause. Some earlier previous studies (e.g., Darby et al., 2016;
77 X. X. Lu & Siew, 2006; Walling, 2008) suggest that, as of the mid-2000s, the effects of dams built on

78 the Chinese part in the 1990s had not significantly affected sediment loads in the lower part of the
79 basin, and specifically the flow of sediment to the delta. However, prior attempts to estimate the
80 impact of planned dams on the sediment load to the delta have suggested that future sediment loads
81 could be significantly affected: Kummu et al. (2010), for example, estimated a sediment load reduction
82 of 51-69% if all planned dams are to be built, while Kondolf et al. (2014) found that the reduction could
83 be as high as 96%. However, previous empirical studies are now outdated, while the existing
84 projections of future sediment loads: (i) focus exclusively on the impacts of damming; (ii) have
85 employed damming databases that do not always identify all relevant infrastructure reliably, and; (iii)
86 do not take into account other drivers, such as anthropogenic climate change.

87 Given the extreme importance of the Mekong delta for the livelihoods of the millions of people living
88 there (Nguyen et al., 2019), and the enormous anthropogenic pressure that the Mekong River has
89 been subject to in recent years, due to river damming and climate change, it is essential to assess
90 accurately the impact of natural and anthropogenic stressors on the sediment flux of the Mekong
91 River. In this paper we provide a comprehensive assessment of the potential impacts of future
92 environmental change on future (to 2100) Suspended Sediment Flux (SSF) to the Mekong delta. We
93 use a dynamic, semi-distributed, catchment model to identify how SSF has changed in the historical
94 period (1980-2020) and will change in the future (2020-2100) throughout the Mekong's large,
95 transboundary, basin, under the combined influence of dam construction and anthropogenic climate
96 change. Importantly, we set the model up using the latest and most comprehensive database of
97 damming available for the Mekong (provided by the Mekong River Commission). The focus of this
98 paper is on the assessment of the influx of sediment to the apex of the delta, and therefore does not
99 consider deltaic processes such as remobilisation by tides or erosion by sea storms.

100 This represents the first study in which the combined effects of climatic change and dam construction
101 on the Mekong's sediment load have been considered. It represents a step towards understanding of
102 the future dynamics of the Mekong River and its delta, both of which are controlled by the evolution
103 of sediment supply. In addition, we seek to attribute projected declines in sediment flux to the
104 countries within which dams are located in the Mekong's transnational catchment, affording an
105 opportunity to focus potential future management interventions.

106 We show that recent past and future changes in SSF are driven primarily by the effects of damming.
107 Specifically, we show that:

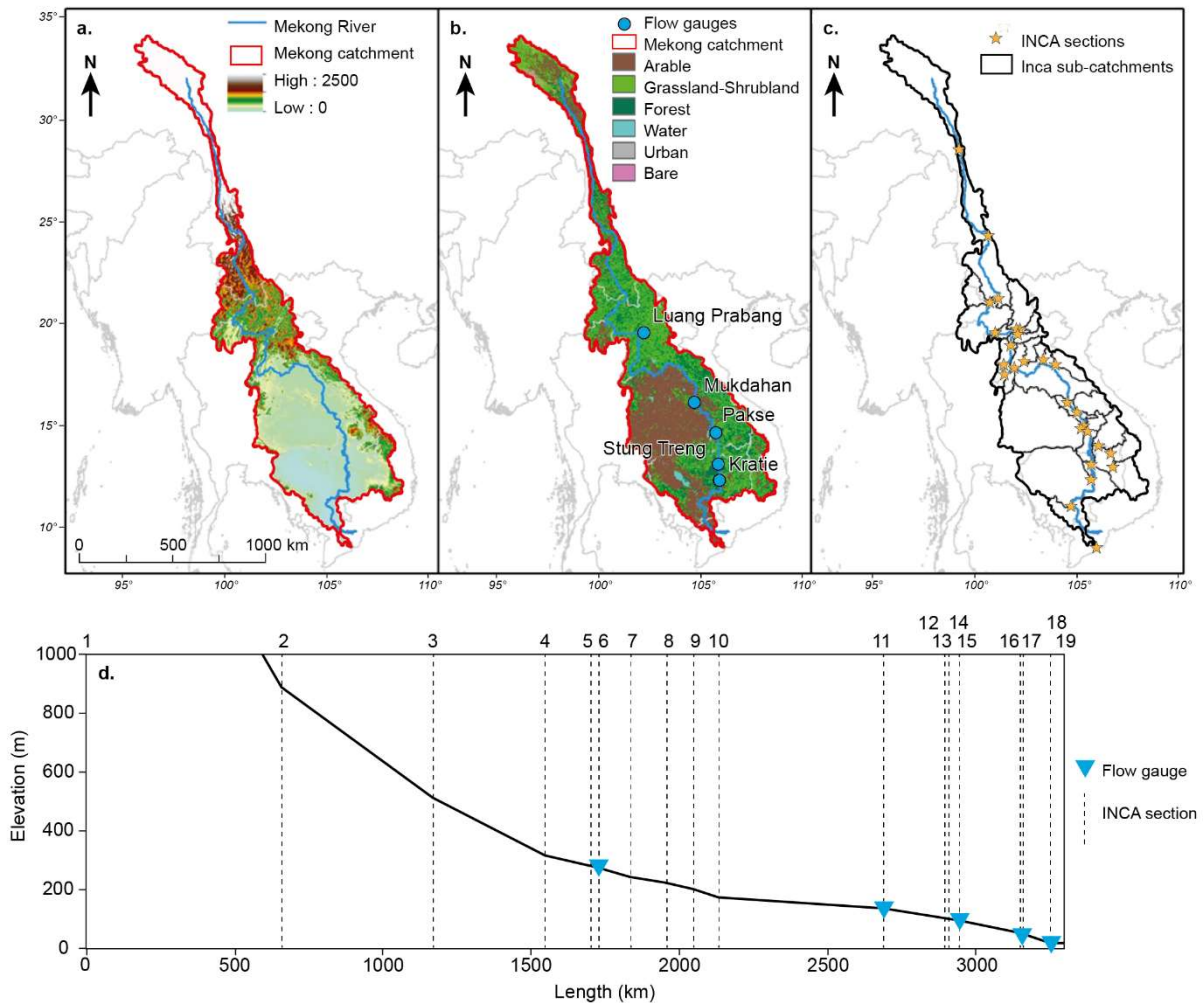
- 108 1. Historical declines (in the period 2000 to 2020) in sediment fluxes to the Mekong delta can be
109 attributed dominantly to dams located in PR China (in 2020, 47% (90% CI: [37%, 54%]) of the
110 total trapped sediment volume is attributed to dams in PR China, mainly due to new dams
111 built in the 2000s and 2010s;
- 112 2. By 2040 the primary cause of the decline in the flow of suspended sediments to the Mekong
113 delta will switch to the numerous dams located in PDR Lao (projected contribution to total
114 trapped volume by 2040: 26% (90% CI: [24%, 28%])) and Cambodia (projected contribution to
115 total trapped volume by 2040: 18% (90% CI: [16%, 19%])).

116

117 **2. Methods**

118 **2.1. The Mekong River**

119 The Mekong River is one of the world’s largest rivers, flowing from the Tibetan Plateau in China to the
 120 South China Sea, crossing PR China, PDR Lao, Myanmar, Thailand, Cambodia and Vietnam on its path.
 121 Its length is approximately 4,350 km and the catchment drainage area is approximately 800,000 km²
 122 (Figure 1A). Figure 1B shows the land use of the catchment, which is dominated by grassland and
 123 forest land in its upper part, and by agricultural land in the lower part. The fraction of urban land is
 124 relatively small (1.5%) compared to the other land uses.



125

126 *Figure 1. A) Mekong catchment extent and elevation. B) Mekong catchment land use and location of the flow gauges. C) INCA*
 127 *sub-catchment and river sections. D) Mekong river profile from section 1 (PR China-Thailand- PDR Lao border) to section 19*
 128 *(river mouth), with INCA section and flow gauge locations.*

129 The annual precipitation is around 1700 mm, but shows strong seasonal variations, with strong
 130 predominance of the rainy southwest monsoon season (Kazama et al., 2007). The upper part of the
 131 catchment is a steep narrow valley primarily determined primarily by Himalayan orogeny (Gupta,
 132 2009). The intermediate part of the catchment, in PDR Lao and Thailand, widens slightly, although it
 133 is still dominated by mountains. Its geology is formed by pre-Tertiary metamorphosed sedimentary
 134 rocks and intruded granites, transitioning towards Quaternary alluvium, mainly fine to coarse sand

135 with some clay and gravel. The lower basin is characterised by a flood plain filled with an alluvium of
136 variable thickness (Gupta, 2009).

137 2.2. The INCA model

138 The INCA (INtegrated CAtchment) model is a semi-distributed, physically-based, hydrological and
139 water quality model, that was initially developed during the 1990s (Whitehead et al., 1998) and which
140 has been updated regularly ever since (Lázár et al., 2010; Lu et al., 2017, 2016; Nizzetto et al., 2016;
141 Wade et al., 2002; Whitehead et al., 2016). In its various guises INCA has been applied to hundreds of
142 catchments all over the world, including on large rivers such as the Ganges in India/Bangladesh
143 (Whitehead et al., 2015) and the Mekong (Whitehead et al., 2019).

144 In this study, the INCA-P 1.4.11 model version was used (henceforth INCA-P; also used in Bussi et al.,
145 2017; Bussi, Dadson, et al., 2016; Bussi, Whitehead, et al., 2016). The structure of the hydrological
146 sub-model in INCA-P is described fully in Wade et al. (2002). In summary, the rainfall-runoff
147 transformation is based on a simple mass balance, dividing hydrologically effective rainfall (i.e., the
148 fraction of rainfall that contributes to flow) into direct runoff, soil water and groundwater, depending
149 on the characteristics of the soil and the aquifer. The stream flow is then routed downstream by means
150 of another mass balance and accounting for the characteristics of the river channel. The catchment
151 under consideration is divided into a series of sub-catchments (for which the land phase parameters
152 can be characterised individually based on land cover), so that these hydrological processes can be
153 computed in a semi-distributed manner. The meteorological inputs required for the model are rainfall
154 and temperature. These variables are used to compute the hydrologically effective rainfall and the soil
155 moisture deficit, which are also required by INCA, by means of another hydrological model, PERSiST
156 (Futter et al., 2014). PERSiST is a semi-distributed rainfall-runoff model specifically designed to
157 compute input series for the INCA model. Other model inputs are topography, land use, point-source
158 effluents (if any), channel width and slope.

159 The sediment transport component of the model is described in Jarritt and Lawrence (2006) and Lázár
160 et al. (2010). A detailed description can also be found in Bussi et al. (2016). This sediment transport
161 component of the INCA model can be divided into two sub-components: the land phase, which
162 reproduces soil erosion and transport processes from the hillslope to the river network, and the
163 channel phase, which simulates entrainment and storage processes within the river channel system.
164 The sediment generation can be triggered by splash detachment, sheet erosion and rill erosion. Soil is
165 eroded from a pool of parental material through the splash detachment and sheet erosion
166 mechanisms and routed downstream to a pool of readily available sediment, which represents the
167 sediment that is available to be transported to the river network. Sediment is classified into five
168 textural classes: clay (0–0.002 mm), silt (0.002–0.06mm), fine sand (0.06–0.2 mm), medium sand (0.2–
169 0.6 mm), and coarse sand (0.6–2mm). The amount of sediment routed to the river network depends
170 on the availability of sediment and the overland flow transport capacity. It should be noted that the
171 model does not account for complete depletion of parent soils (because the parent material to be
172 eroded is unlimited), but it does compute a balance between sediment availability and overland flow
173 transport capacity in order to calculate the sediment mass to be transported downstream. The
174 representation of the hillslope sediment cycle is therefore both transport-limited and supply-limited.
175 The model accounts for the characteristics of the soil, the land use and the connectivity between
176 slopes and channels.

177 Once in the main river network, sediment is routed downstream as a function of the river transport
178 capacity, which is computed separately for a range of texture classes using the Bagnold (1966) stream
179 power equation. The transport capacity is used to split the material that enters the river reach into
180 deposited and suspended, and to transfer the suspended part downstream. Depending on the size of
181 the sediment and the transport capacity, the material can deposit into the riverbed and accumulate
182 or be routed downstream. At the same time, again depending on the transport capacity and on
183 sediment availability, deposited sediment can also be re-entrained. The balance between sediment
184 availability and river flow transport capacity is also accounted for at the reach scale, thus providing a
185 representation of the river sediment cycle which is both transport-limited and supply-limited,
186 depending on a variety of factors such as climate, soils, land use, slope, etc. Background release of
187 material (i.e., bank erosion) is also computed in a simplified way as a non-linear function of the river
188 flow.

189 The INCA model does consider sediment deposition and re-entrainment within the river channel and
190 allows for reproducing both transport-limited and supply-limited sediment transport. However, the
191 INCA model is a catchment and river sediment model and does not consider long-term morphological
192 changes to the river channel (other than sediment deposition or sediment depletion). This
193 simplification is usually accepted in river sediment modelling because of the relatively short time
194 period that is typically modelled, during which it is assumed that any geomorphological change will be
195 negligible compared to other in-stream processes. The spatial scale is also relevant: in large-scale
196 applications, local geomorphological changes might be negligible, while in small-scale application this
197 might not be true. In the present study, we model more than 100 years over a large area. It can be
198 assumed that no significant changes to the riverbed morphology are expected aside from deposition
199 and remobilisation within this time frame and at this scale, especially because many previous studies
200 point out that many sections of the river are bedrock-constrained (Carling et al., 2019; Kondolf et al.,
201 2014; Meshkova and Carling, 2012; Nie et al., 2018; Van et al., 2012) and thus significant
202 geomorphological changes are expected to take much more than just a century. This might not be
203 true for the delta part of the river, however, as pointed out previously, this paper focuses on the inland
204 part of the river and estimates the influx of sediment at the apex of the delta.

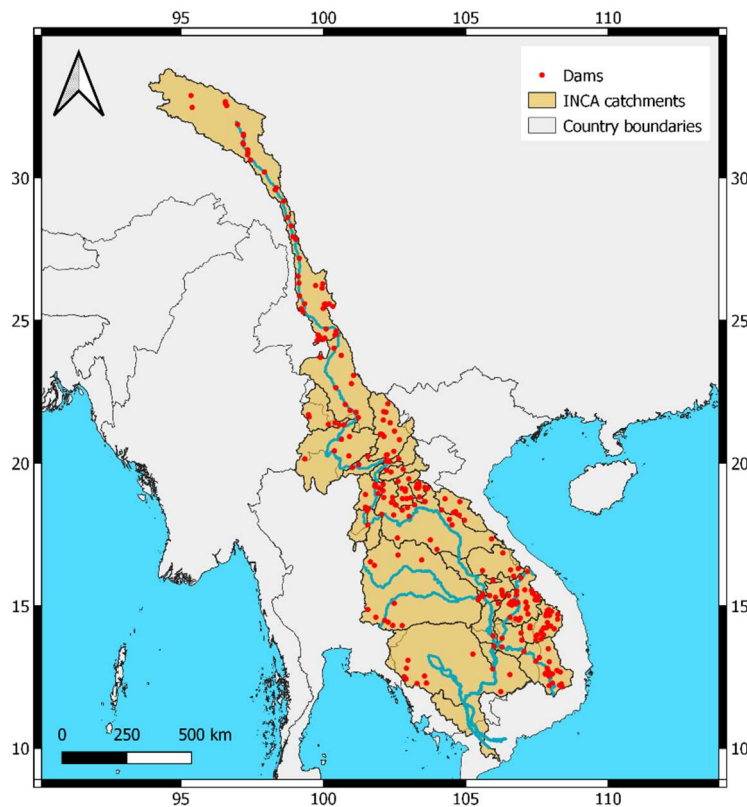
205 2.3. Data, model set-up and model calibration

206 Daily observed precipitation and temperature data were obtained from a network of several local
207 stations. In particular, the Ministry of Water Resources and Meteorology of Cambodia provided 21
208 daily precipitation stations and 14 monthly temperature station, the KNMI's (Dutch met office)
209 Climate Explorer platform another 14 precipitation and temperature stations within or adjacent to the
210 Mekong delta (part of the Global Historical Climatology Network and managed by the corresponding
211 national meteorological services), and the US National Climate Data Center 17 precipitation and
212 temperature stations in PR China, 5 in PDR Lao and 24 in Thailand. These data were quality-controlled
213 and processed to obtain daily precipitation and temperature time-series for the period from 1975 to
214 2016, covering the whole Mekong catchment. Land use data were obtained from the European Space
215 Agency's GlobCover product (Bontemps et al., 2011), which maps the 2009 global land cover at 300 m
216 resolution. The land use classes were aggregated into six classes: arable, grassland-shrubland, forest,
217 urban and bare. Elevation maps were obtained from the Shuttle Radar Topography Mission (Farr et
218 al., 2007) at a resolution of 90 m and were used to compute river reach lengths, sub-catchment
219 extensions and reach slopes. Flow data used for model calibration and validation were obtained from

220 hydrological records archived in the Mekong River Commission data portal. In this study, data from
221 1981 to 2005 were used, as in Darby et al. (2016). Daily sediment flux data for the same period were
222 derived from Darby et al. (2016) (Figure 1B and Figure 1D).

223 Daily precipitation and temperature data from a climate model were employed to project changes in
224 the future climate. The PRECIS Regional Circulation Model coupled to the GFDL-CM Global Circulation
225 Model was employed in this study (Thuc et al., 2016; Whitehead et al., 2019). The Representative
226 Concentration Pathways (RCPs) 4.5 and 8.5 were used to drive the climate model (Edenhofer et al.,
227 2014; Janes et al., 2019). RCP 8.5 reproduces greenhouse gas emissions rising continuously throughout
228 the 21st century and represents a relatively challenging situation. Emissions in RCP 4.5 peak around
229 2040, then decline. The results of the climate model were bias-corrected, applying a quantile mapping
230 correction (Lafon et al., 2013) to reproduce the observed climate. These climate scenarios allow
231 climate changes to be projected up to the year 2100.

232 A database of existing and planned dams was obtained from the Mekong River Commission. A total of
233 284 dams were identified, 30 of which are located on the main stem of the Mekong (7 of them are
234 already in place), and the rest on tributaries (Figure 2). This database includes information on reservoir
235 volume and year of construction (or planned year of construction). Around 130 dams exist at the
236 moment, the rest are either under construction or planned. The trapping effect of the dams was
237 reproduced by introducing short river reaches in the model structure just upstream of the dam
238 locations. In these reaches, the model sediment transport capacity parameters were adjusted such
239 that the long-term ratio between the sediment volume flowing out of the reach and the sediment
240 volume flowing into the reach was equal to the trap efficiency of the reservoirs within the reach, the
241 latter as computed according to Brune (1953). The method developed by Brune (1953) relates the
242 sediment trap efficiency, i.e. the ratio of the sediment mass trapped by a dam to the total sediment
243 mass transported by the river to the dam, to the ratio of the reservoir volume and the annual average
244 inflow. This method also allows consideration of the behaviour of particles with different sizes in
245 reservoirs. INCA is in fact set up to reproduce five textural classes: clay (0–0.002 mm), silt (0.002–
246 0.06mm), fine sand (0.06–0.2 mm), medium sand (0.2–0.6 mm), and coarse sand (0.6–2mm), and a
247 maximum entrainable grain size is computed for each reach and each time-step based on the transport
248 capacity equation. In the reaches where reservoirs are set up, this procedure mimics the trapping
249 mechanisms of reservoirs: during low flows particles of all sizes settle, while during high flows fine
250 particles are only partially trapped while coarse particles still mostly deposit. Changes in reservoir
251 volume and hence trapping efficiency were modelled at a decadal disaggregation level, i.e., different
252 trap efficiency values were computed for every decade from 1980 to 2100, based on the total reservoir
253 volume at the end of each decade (in the case of historical decades) or the future damming scenario
254 (in the case of future decades).



255

256 *Figure 2. Spatial distribution of dams within the Mekong catchment.*

257 Figure 1B shows the location of the flow gauges used for model calibration, namely: Luang Prabang
 258 (INCA reach 6), Mukdahan (reach 11), Pakse (reach 14), Stung Treng (reach 16) and Kratie (reach 17),
 259 with Figure 1C illustrating the extent of the sub-catchments employed here. Figure 1D shows a
 260 longitudinal profile of the river, extending from the source (reach 1) to the river mouth. The locations
 261 of the 19 main stem reach sections used in the INCA representation of the Mekong system and the
 262 flow gauges are also shown (the 11 other reach sections are set on tributaries). The coordinates and
 263 characteristics of the model reaches and their corresponding sub-catchments are reported in Table S6
 264 in the Supplementary Material. The accumulated reservoir volume by INCA sub-catchment (Mm³)
 265 variation in time is shown in Table 1.

266 *Table 1. Accumulated reservoir volume by INCA sub-catchment (Mm³) and by decade.*

INCA ID	Name of the reach	1950	1960	1970	1980	1990	2000	2010	2020	2030
1	Gushui	0	0	0	0	0	0	0	4333	17490
2	Manwan	0	0	335	494	2506	2506	23723	24762	24762
3	Ban Mau	1490	1490	1490	1490	1490	3520	27223	27223	27800
4	Pak Beng	0	0	0	0	0	0	4178	8825	8825
5	Luang Prabang	0	0	0	0	0	0	4168	4168	5757
6	Luang Prabang Gauge	0	0	0	0	0	0	1023	5521	5885
7	Xayabouri	0	0	0	0	0	0	2026	2026	2026
8	Pak Lay	0	0	0	0	0	0	473	2016	6227
9	Sanakham	0	0	0	0	0	0	0	282	282
10	Santhong-Pakchom	0	0	0	0	0	0	0	1097	1097
11	Mukdahan	0	166	686	799	799	984	1282	3604	3604
12	Ban Kum	0	0	0	0	0	0	0	2188	4298
13	Latsua	0	0	0	0	225	225	225	2302	2302
14	Pakse	0	0	0	0	0	0	0	0	0
15	Stung Treng	0	0	0	0	0	0	0	0	669
16	Stung Treng Gauge	0	0	0	0	0	0	1793	1793	1927
17	Sambor-Kratie	0	0	0	0	0	0	0	3794	3794

18	Phnom Penh	0	0	110	110	110	110	225	225	951
19	River mouth	0	0	0	0	0	0	0	0	0
20	Nam Loi	0	0	0	0	0	0	1755	3093	3823
21	Nam Suong	0	0	0	0	0	0	0	4072	4072
22	Nam Khan	0	0	0	0	0	0	4791	4791	4791
23	Nam Ngum	0	0	4700	4700	4700	4700	8987	11251	11251
24	Nam Nhiep	0	0	0	0	0	0	2984	3127	3127
25	Nam Cadinh	0	0	0	0	0	0	8430	19099	19299
26	Se Bang Hieng	0	0	0	0	0	0	540	2238	2238
27	Nam Mun	0	4009	6451	7017	7017	7017	7017	7017	7017
28	Se Kong	0	0	0	0	3530	3530	17663	25458	25956
29	Se San	0	0	0	0	1073	2122	3332	3332	5785
30	Sre Pok	0	0	0	0	0	933	1152	1152	3026

267

268 Since INCA is not a fully distributed model, dams cannot be introduced at any location, and they must
269 coincide with the position of the downstream section of a reach. With the aim of achieving a
270 reasonably simple model set-up while at the same time maximising the model performance, dams
271 with a reservoir volume smaller than 100 Mm³ (i.e., 124 dams in total) were not considered in this
272 study. This is not a major limitation as these 124 small dams together account for less than 2% of the
273 total reservoir storage volume in the Mekong cascade. The remaining 155 dams, which have a total
274 reservoir storage volume of 208,000 Mm³, were assigned to a corresponding model reach based on
275 their geographical location. The location of the downstream sections of the model reaches was
276 carefully selected in order to match the location of the largest reservoirs (see Figure 2). While the
277 model reach sections of the main stem were specifically designed so that their corresponding sub-
278 catchments contained only one dam per reach, the tributary sub-catchments often contained more
279 than one dam. In these cases, an equivalent reservoir volume was computed as the sum of all the
280 reservoir volumes falling within the sub-catchment and this value was then used to compute a sub-
281 catchment trap efficiency by means of the Brune (1953) method. A discussion of this assumption is
282 reported in the Supplementary Material.

283 The INCA model was calibrated by means of a Monte Carlo calibration procedure, according to the
284 following steps. First, the most influential parameters were identified and a feasibility range for their
285 values was estimated, based on previous applications of the model in other catchments. A list of the
286 calibrated parameters is reported in Table 2, together with the corresponding feasibility range. A
287 description of the parameters and their physical meaning is provided in Wade et al. (2002) and Bussi
288 et al. (2016). Second, a large set of parameter values (50,000) was generated randomly from uniform
289 distributions within the defined feasibility ranges for each parameter. Third, the model was run with
290 each parameter set and results were obtained. Fourth, all the results were analysed and the Kling-
291 Gupta Efficiency index, or KGE (Gupta et al., 2009), was computed through comparison of observed
292 and simulated daily flow and sediment flux time series, for locations where both flow and sediment
293 records were available. Finally, a small number (15) of parameter sets was selected based on their
294 performance and used to conduct the simulations described in this paper. The number of parameter
295 sets to be used was chosen as a compromise between parameter set performance and computational
296 burden.

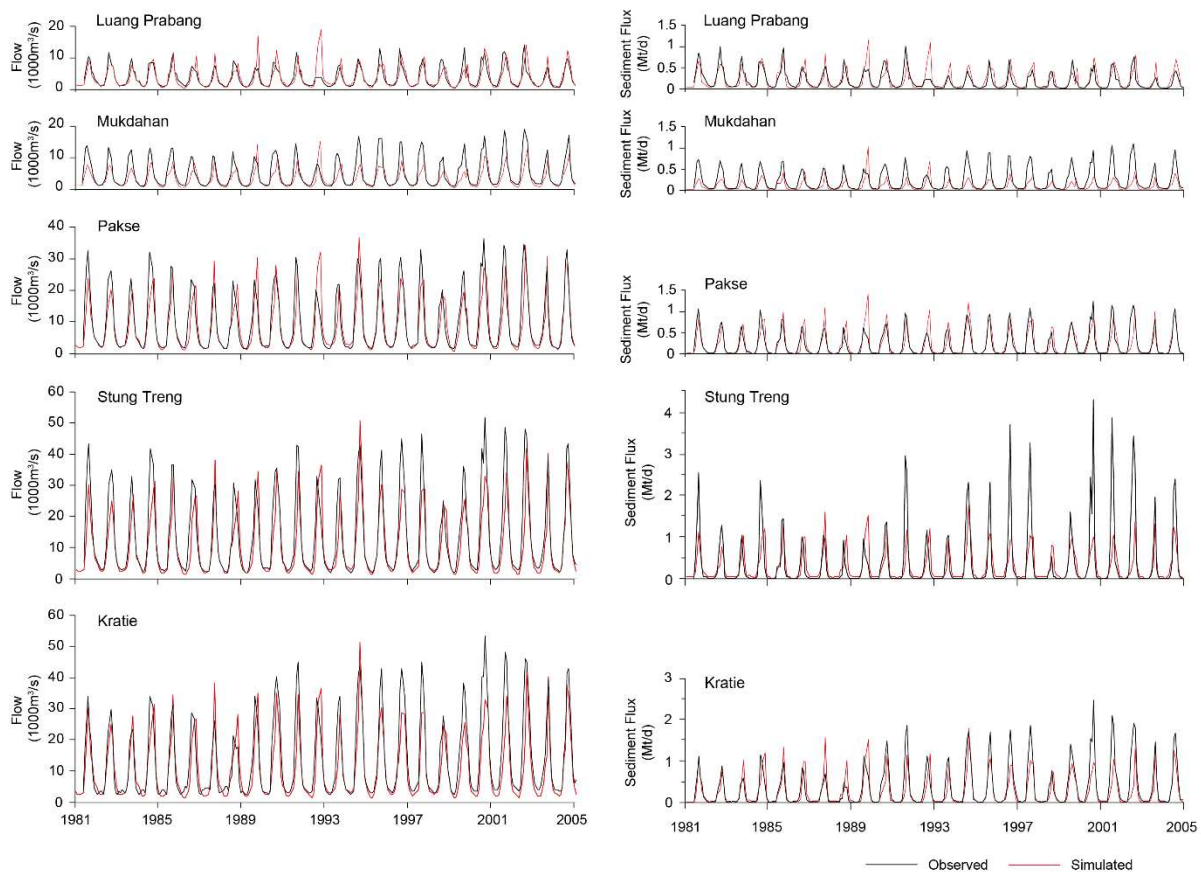
297 *Table 2. Calibrated model parameters and feasibility ranges.*

Parameter type	Parameter name	Minimum value	Maximum value
catchment	Base Flow Index	0.6	0.95
reach	Flow a	0.02	0.1
reach	a8 (river transport capacity parameter)	0.00001	0.001

reach	a9 (river transport capacity parameter)	0.00001	0.001
catchment	groundwater zone time constant	30	80
catchment	rainfall excess proportion	0.05	0.2
catchment	threshold soil zone flow	0.01	0.1
catchment	transport capacity non-linear coefficient	0.2	0.8
catchment	transport capacity scaling factor	0.2	0.7
land	direct runoff time constant	1.5	2.5
land	flow erosion soil erodibility parameter (arable)	0.6	2.4
land	flow erosion soil erodibility parameter (grassland)	0.3	1.2
land	flow erosion soil erodibility parameter (forest)	0.3	1.2
land	flow erosion soil erodibility parameter (wetland)	0.1	0.5
land	flow erosion soil erodibility parameter (urban)	0.1	0.5
land	flow erosion soil erodibility parameter (bare)	5	20
land	soil reactive zone time constant	5	9
land	splash detachment soil erodibility parameter (arable)	0.9	3.5
land	splash detachment soil erodibility parameter (grassland)	0.35	1.5
land	splash detachment soil erodibility parameter (forest)	0.35	1.5
land	splash detachment soil erodibility parameter (wetland)	0.07	0.3
land	splash detachment soil erodibility parameter (urban)	0.07	0.3
land	splash detachment soil erodibility parameter (bare)	8	35

298

299 The INCA model was calibrated over the time period 1981-1989 (inclusive) and validated over the
300 period 1990-2005 (inclusive). Comparisons of simulated and observed flows and sediment loads for
301 all the five gauged sections investigated here, expressed in terms of monthly flow and monthly
302 Suspended Sediment Flux (SSF), are shown in Figure 3 (the model calibration and validation was
303 undertaken using daily flows and SSFs, but the data reported in Figure 3 are aggregated to monthly
304 resolution for the purpose of aiding clarity of visualisation). The daily flow and suspended sediment
305 flux KGEs obtained by the model are shown in Table 3.



306

307 *Figure 3. Calibration and validation results (monthly flow and monthly sediment flux) at five locations on the Mekong River*
 308 *(Luang Prabang, Mukdahan, Pakse, Stung Treng and Kratie).*

309 *Table 3. Kling-Gupta Efficiency (KGE) ranges obtained by the INCA model (ensemble of 15 parameter sets) computed on daily*
 310 *flow and monthly suspended sediment flux for the calibration (1980-1989) and validation (1990-2005) periods.*

Time period	Variable	Luang Prabang	Mukdahan	Pakse	Stung Treng	Kratie
1980-1989	Flow	0.59-0.74	0.41-0.54	0.66-0.77	0.61-0.71	0.75-0.83
1980-1989	Suspended sediment flux	0.45-0.71	0.17-0.35	0.38-0.73	0.41-0.48	0.37-0.7
1990-2005	Flow	0.51-0.6	0.31-0.44	0.7-0.8	0.62-0.72	0.59-0.67
1990-2005	Suspended sediment flux	0.13-0.58	0.03-0.23	0.59-0.78	0.21-0.33	0.45-0.62

311

312 2.4. Model scenarios

313 Here we investigated two climate change scenarios (corresponding to the RCP4.5 and RCP8.5
 314 emissions scenarios, see for example Busico et al., 2019), and four damming scenarios: A) considering
 315 all dams built before 2010; B) considering all dams built or under construction before 2020; C)
 316 considering all dams planned for the near future (i.e., from 2021 to 2030); D) considering all dams
 317 planned for the far future (i.e., from 2031 onwards). In particular, all combinations of these climate
 318 and damming scenario were considered, as shown in Table 4.

319 *Table 4. Scenarios considered in this study.*

Damming scenario	Baseline climate	Future climate (RCP4.5)	Future climate (RCP8.5)
A) considering all dams built before 2010	<i>Baseline A</i>	<i>RCP4.5 A</i>	<i>RCP8.5 A</i>
B) considering all dams built or under construction before 2020	<i>Baseline B</i>	<i>RCP4.5 B</i>	<i>RCP8.5 B</i>
C) considering all dams planned for the near future (i.e., from 2021 to 2030)	<i>Baseline C</i>	<i>RCP4.5 C</i>	<i>RCP8.5 C</i>
D) considering all dams planned for the far future (i.e., from 2031 onwards)	<i>Baseline D</i>	<i>RCP4.5 D</i>	<i>RCP8.5 D</i>

320

321 In all scenarios, the same ensemble of 15 model parameter sets was used (i.e., the 15 model
 322 parameter sets that gave the best KGE values for the daily SSF in the calibration stage), therefore
 323 obtaining a range of future sediment transport estimates rather than a single value.

324 3. Results

325 The results were analysed in terms of absolute value of SSF at different sections (the gauged sections
 326 were used as reference locations, i.e., Luang Prabang, Mukdahan, Pakse, Stung Treng and Kratie) and
 327 in terms of SSF variations compared to the baseline scenario (baseline climate, damming scenario A).
 328 Furthermore, the sediment decline caused by dams was attributed to different clusters of dams within
 329 each country in which they are located (including a “transboundary” cluster, for dams that lie on the
 330 border between two countries).

331 The model simulations estimate that the long-term Suspended Sediment Flux (SSF), as computed for
 332 the time period 1980-2009 (thus considering damming scenario A for the historical period), is 68.3 [60,
 333 77.9] Mt/y, 34.3 [29.7, 39.5] Mt/y, 83.9 [76.3, 90.3] Mt/y, 98.7 [93.4, 103.2] Mt/y and 98.6 [93.4,
 334 103.2] Mt/y for the stations at Luang Prabang, Mukdahan, Pakse, Stung Treng and Kratie, respectively
 335 (the confidence interval indicates the 90% CI, based on the INCA model ensemble results). However,

336 these values vary in time, mainly depending on climate variability and the construction of new dams,
 337 as shown in Table 5, where the SSFs of the same five sections are reported by decade.

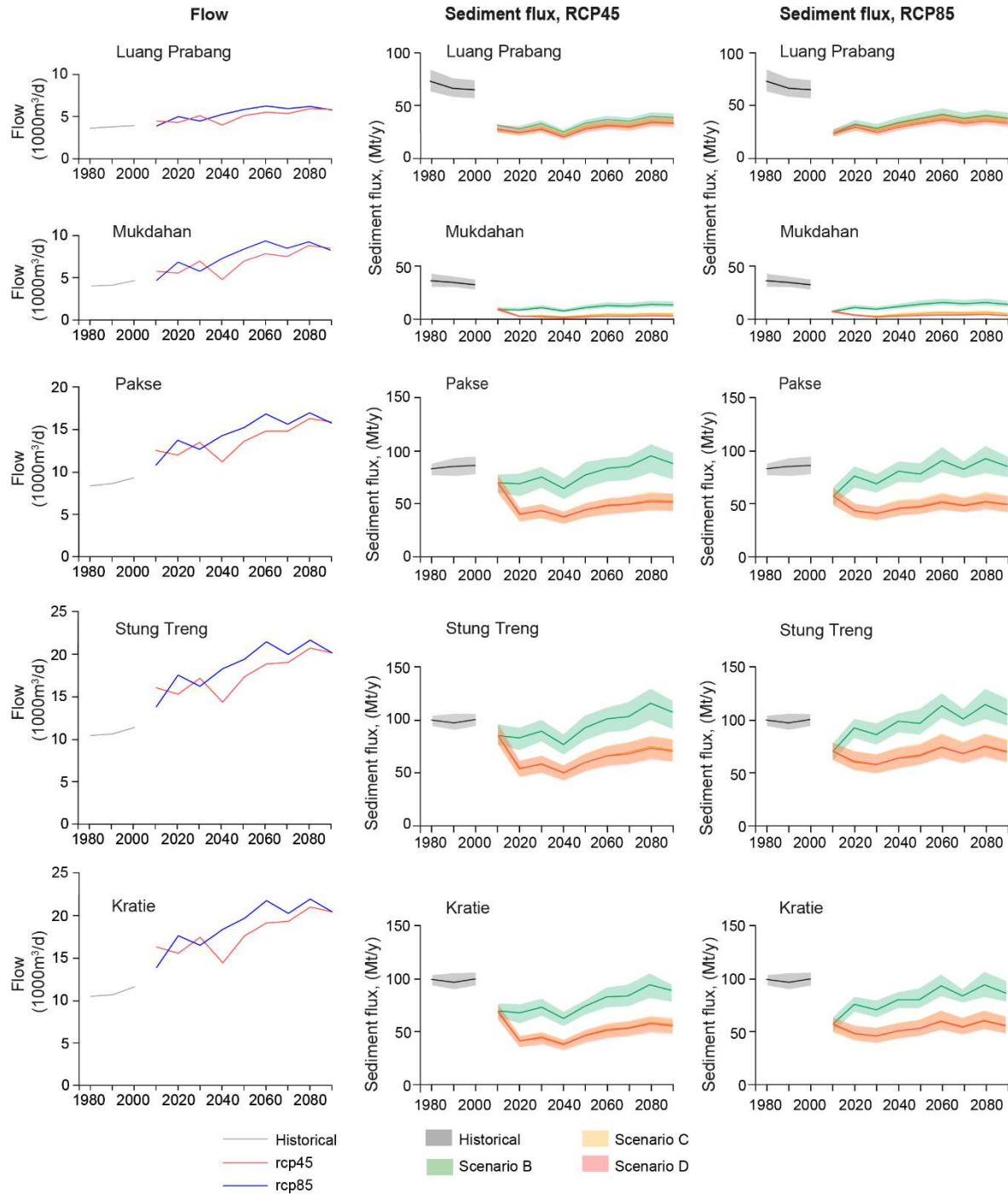
338 *Table 5. Suspended sediment flux (Mt/y) at five locations on the Mekong by decade. The values in the brackets show the 90%
 339 CI.*

Decade	Reach 06 (Luang Prabang)	Reach 11 (Mukdahan)	Reach 14 (Pakse)	Reach 16 (Stung Treng)	Reach 17 (Kratie)
1980s	72.9 [63.7, 84.2]	36.1 [30.3, 42.2]	82.0 [75.9, 87.0]	99.4 [93.6, 104.3]	99.3 [93.5, 103.8]
1990s	66.8 [58.8, 76.6]	34.5 [30.3, 40.0]	84.3 [75.6, 92.3]	96.7 [90.3, 105.5]	96.6 [90.3, 105.3]
2000s	65.1 [57.4, 74.2]	32.4 [28.4, 37.6]	85.3 [77.2, 94.1]	100.0 [93.4, 105.1]	99.9 [93.6, 105.4]

340

341 The results of the INCA model driven by future climatic scenarios are shown in Figure 4 (please note
 342 that what appears to be a discontinuity in the SSF between the historical period and future period is
 343 in reality an effect of the decadal aggregation of the model results and the fact that between the
 344 historical and the future periods the total reservoir volume increased greatly). Figure 4 suggests that
 345 under RCP8.5 the increase in flow should occur earlier in time than under RCP4.5. For example, the
 346 model results indicate that the average flow is expected to reach 20,000 m³/s at Kratie by the 2050s
 347 under the RCP8.5 scenario, but not until the 2070s-2080s under the RCP4.5 scenario.

348 Similar increases are indicated also in terms of SSF. However, the simulated impact of dams on
 349 sediment transport is greater than the impact of climate change. The dams built in the last decade
 350 (2010-2020, scenario B) are projected to reduce SSF to 44%, 30%, 86%, 88% and 71% of the SSF values
 351 simulated in the 2000s (scenario A) at Luang Prabang, Mukdahan, Pakse, Stung Treng and Kratie,
 352 respectively (with the projected future values of SSF being 30, 13, 87, 107 and 87 Mt/y respectively,
 353 computed as the average of the 2030-2060 period under RCP4.5 emissions). The dams planned for the
 354 near future (2020-2030, scenario C) are projected to further lower the simulated SSFs to 40%, 11%,
 355 50%, 57% and 46% of their values in 2000 (with the projected future values of SSF being 27, 4, 42, 57
 356 and 45 Mt/y respectively), while the dams planned for the far future (scenario D) reduce the SSF
 357 further still to 38%, 7%, 49%, 57% and 44% of the levels of the 2000s (with the projected future values
 358 of SSF being 26, 2, 41, 56 and 45 Mt/y respectively).

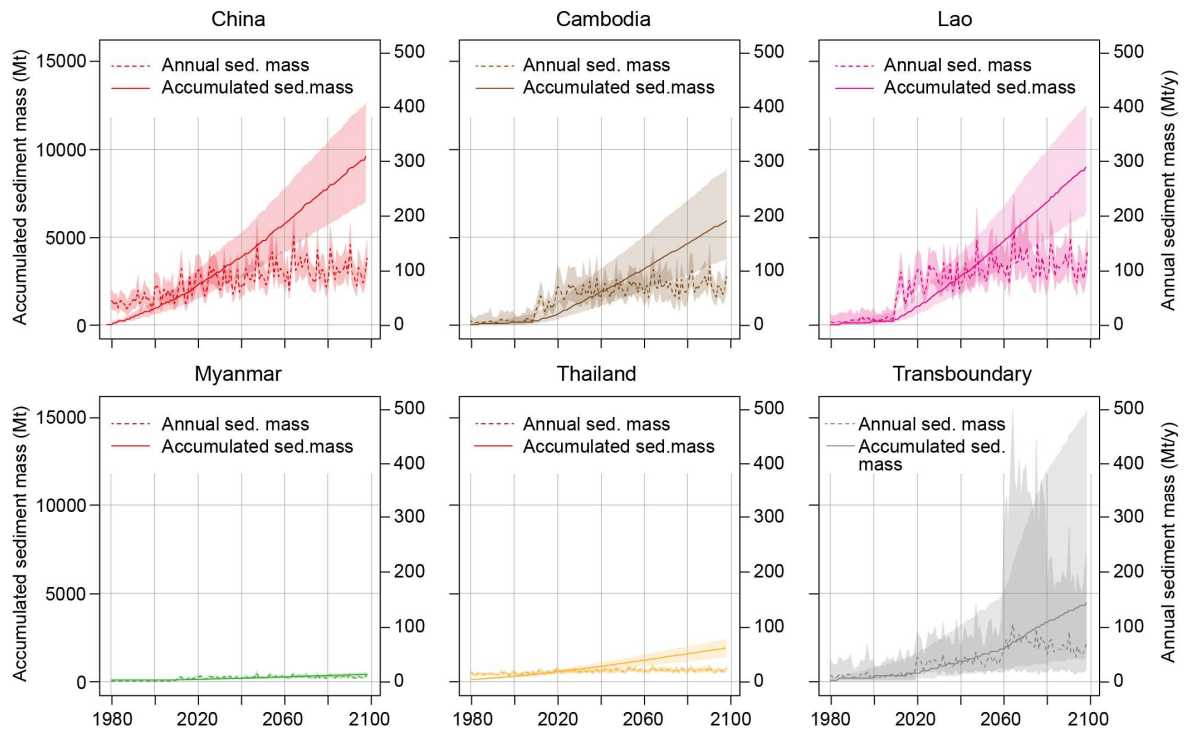


359

360 *Figure 4. Flow and suspended sediment flux (SSF) projections driven by the GFDL climate model results under two RCP and*
 361 *three damming scenarios: B) considering all dams built before 2020 or under construction; C) considering all dams planned*
 362 *for the near future (i.e., up to 2030); D) considering all dams planned for the far future (i.e., after 2030). Scenario A*
 363 *(considering only dams built before 2010) is not projected into the future as is not feasible anymore. Note that the suspended*
 364 *sediment flux curves under scenarios C and D partially overlap. The shaded areas represent the 90% CI.*

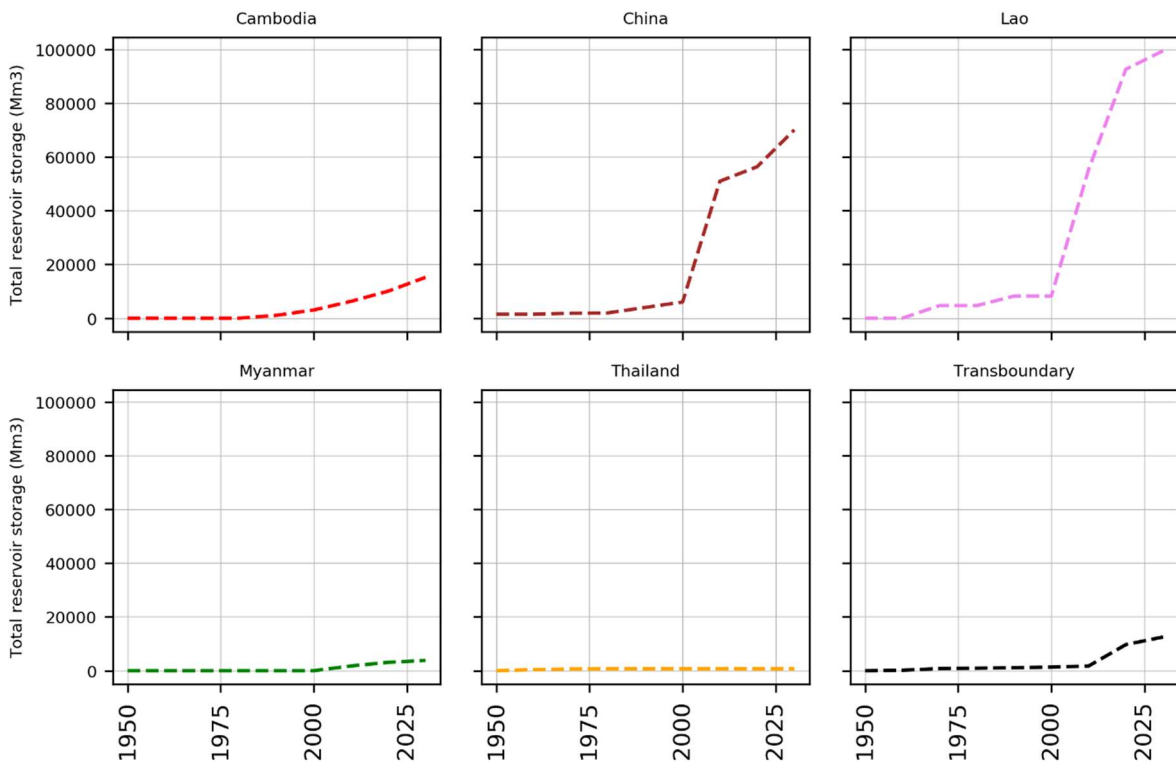
365 Figure 5 provides a visualisation of the variation of the annual trapped sediment mass, and the
 366 cumulative, increase in sediment mass trapped behind the dams, for the period from 1980 to 2100,
 367 as projected by INCA under the RCP8.5 scenario for all constructed and planned dams (i.e., Scenario
 368 D from Figure 4). In this diagram the results are grouped to show the accumulated impact of trapping
 369 behind dams located in each of the Mekong's countries. Note that a total of 7 dams are located on

370 the border between two countries (PDR Lao-Cambodia or PDR Lao-Thailand) and these are shown in
 371 the “Transboundary” category (lower right panel in Figure 5). For reference, Figure 6 shows the
 372 variation in time of the total reservoir storage per country.



373

374 *Figure 5. Annual and accumulated sediment mass trapped in reservoirs starting from 1980, grouped by country, under RCP8.5*
 375 *and assuming that all planned dams are built (scenario D). Reservoirs built on the border of two countries are grouped in the*
 376 *“Transboundary” category. The shaded areas represent the 90% CI.*



377

378 *Figure 6. Evolution of the total reservoir storage per country (2020 and 2030 levels are projections).*

379 4. Discussion

380 Although previous studies (Kondolf et al., 2014; Kummu et al., 2010) have sought to quantify the
381 impact of damming on the suspended sediment load of the Mekong River, to date none have
382 considered the combined impacts of damming and human-induced changes in climate. In this study
383 we demonstrate that these two drivers of change have opposing impacts on the Mekong's future
384 suspended sediment load. However, although anthropogenic climate change is expected to increase
385 river flows and suspended sediment fluxes to the delta, the climate-driven uplift in future sediment
386 flux is not large enough to fully compensate for sediment retention by dams and reservoirs.

387 The climatic projections used in this study indicate that mean annual average temperature over the
388 Mekong catchment is expected to increase by between 2 (RCP4.5) and 3 (RCP8.5) degrees Celsius by
389 the 2060s. Precipitation is also expected to increase, especially during the rainy season, by 10% in
390 2030-2060 and by 26% in 2060-2090 under the RCP4.5 scenario. The RCP8.5 projections predict a
391 similar, but slightly larger, increase of precipitation. The combined effect of these changes on INCA
392 simulated flows is an increase in the mean annual river flow, of up to 70% compared to current values
393 at Kratie (which is located close to the apex of the delta), as shown in Figure 4. Climate change is
394 therefore expected to increase flows towards the delta, consistent with Wang et al. (2017), who also
395 projected a sharp increase in flood magnitude in the Mekong.

396 Regarding future fluxes of sediment, our study suggests that the mean annual Suspended Sediment
397 Flux (SSF) to the Mekong delta (as computed at Kratie), has recently (1980-2009) been as high as 99
398 (93-103) Mt/y. This INCA-derived estimate of the near-contemporary SSF is broadly consistent with
399 previous estimates derived from measurements, such as those of Darby et al. (2016) (87.4±28.7 Mt/y,
400 computed also at Kratie, for the time period 1981-2005); Kummu & Varis (2007) (81 Mt/y at Kratie,
401 over the time period 1995-2000) and X. Lu et al. (2014) (113 Mt/y at Pakse, 400 km upstream of Kratie,
402 over the time period 1993-2000).

403 What our study highlights, however, is that rapid changes within the Mekong catchment have in effect
404 rendered these prior empirical estimates of SSF redundant. In particular, the rapid increase in
405 damming intensity in the first and second decades of the 21st century (the total storage of the Mekong
406 catchment dams was 22,200 Mm³ in 2000, 46,300 Mm³ in 2010 and will reach 147,000 Mm³ in 2020)
407 are reflected in a major transition in the Mekong's SSF in the same period. Specifically, in the upper
408 part of the catchment (Luang Prabang), SSF was 68 [60, 78] Mt/year for the period 1980-2009, but is
409 projected to decrease to 26 [23, 30] Mt/year for the 2010-2019 decade and 24 [21, 28] Mt/year for
410 the 2020-2029 decade, under the RCP4.5 scenario. In the long term (2070-2099), SSF at Luang Prabang
411 is expected to recover slightly, up to 38 [33, 43] Mt/yr. At Kratie, SSF is projected to decrease from 99
412 [93, 103] Mt/y during the 1980-2009 period to 46 [40, 51] Mt/yr for the 2010-2019 decade and 43 [37,
413 47] Mt/year for 2020-2029, under the RCP4.5 scenario (decreases of 53% and 57%, respectively, since
414 1980-2009).

415 In the long term (2070-2099), SSF at Kratie is, as the effects of anthropogenic climate change become
416 relatively more pronounced as the century progresses, expected to recover slightly to 62 [56, 68]
417 Mt/year, i.e. around two thirds of what it was in 1980-2009. Nevertheless, the scale of reduction in
418 sediment load is still substantial, reinforcing recent work that highlights how the opportunity to

419 manage the Mekong's dam portfolio to limit the adverse potential for sediment trapping is already
420 severely constrained (Schmitt et al., 2019).

421 As noted above, our findings also highlight that, according to the climate scenarios, SSF should recover
422 in the longer term, although not enough to attain the levels of the recent (1980-2009) period. At Luang
423 Prabang, SSF should increase by 26% (compared to 2010-2029 levels) by 2070-2099 under the RCP4.5
424 scenario and by 38% under the RCP8.5 scenario. At Kratie, these figures are 27% and 31%, respectively.
425 Figure 4 summarises this situation: if no more dams are built (scenario B; unlikely), SSFs should be able
426 to recover to past levels towards the end of the century in the downstream part of the catchment
427 (Pakse, Stung Treng, Kratie), but should not be able to recover in the upstream part (Luang Prabang,
428 Mukdahan). However, if all planned dams are built, the lower Mekong catchment will also experience
429 a long-term decline in sediment fluxes, with significant implications on livelihoods in the delta.

430 It must be highlighted that for a comprehensive analysis of the delta dynamics, all the component of
431 the delta sediment balance should be considered, including inputs from upstream, wave and tide
432 erosion, subsidence, etc. This paper focuses on a single component of this balance, the inflow from
433 the river. The results of the present study certainly contribute to the understanding of the whole
434 sediment balance in the delta and are fundamental for the quantification of its sediment inputs.
435 However, other processes occur in the delta that might play a relevant role and were not within the
436 scope of the present study.

437 5. Conclusion

438 In this study, the impact of sediment trapping caused by damming and of climate change on the
439 sediment fluxes of the Mekong River was quantified. This paper provides the first joint damming-
440 climate change impact assessment for the Mekong River, filling the gaps of previous studies. The
441 results suggest that the rapid increase in damming intensity in the first and second decades of the 21st
442 century will have a major effect on the supply of sediment transmitted through the Mekong River..
443 Specifically, the suspended sediment flux in the lower Mekong is expected to change from 99 [93, 103]
444 Mt/y to 43 [37, 47] Mt/year by 2020-2029 (57% decrease). Our simulations highlight that these
445 declines will not be recovered, despite a projected increase in runoff and sediment transport towards
446 the end of the century, as a consequence of climate change.

447 The major declines in suspended sediment loads and associated problems that our INCA projections
448 indicate have already started to manifest in the last two decades. Our simulations highlight that these
449 declines will not be recovered despite a projected increase in runoff and sediment transport by 2100
450 caused by climate change. Thus, they present a major challenge for sustainable development across
451 the Mekong basin. For example in the upper reaches of the Lower Mekong Basin (at stations such as
452 Luang Prabang and Pakse), declining sediment loads are likely to result in in-channel erosion, with
453 potential adverse impacts on riparian communities and infrastructure, as sediment starved waters
454 released from dams remobilise sediments stored in the Mekong floodplains (Kondolf, 1997). Further
455 downstream, the dramatic decline of SSF delivered from the Lower Mekong (Kratie) presents an
456 existential threat to the Mekong delta. Fluvial sediment deposition on the delta plains, is the only
457 mechanism capable to offset the effects of relative sea-level rise and is very likely to decline.
458 Moreover, a deficit in sediment deposition also threatens the sustainability of agricultural systems
459 and local livelihoods in the delta.

460 Our results highlight how these local impacts arise from the effects of dams located in distinctive
461 upstream jurisdictions in this transnational basin. Our results show that by 2020 47% of the total
462 retained sediment mass was trapped by dams built in PR China, 13% by dams in Cambodia and 21%
463 by dams in PDR Lao, however these figures will change to 35%, 19% and 27%, respectively by 2050, if
464 all planned dams are built. Transboundary dams, mostly built on the PDR Lao–Cambodia and PDR Lao
465 – Thailand borders, are projected to trap 10% of the total trapped sediment by 2050. It is clear that
466 efforts to mitigate severe reductions in SSF will require effective cooperation and governance across
467 borders.

468 Acknowledgments

469 The research reported here was supported by awards BB/P022693/1 and NE/S002847/1 from the
470 Biotechnology and Biological Sciences Research Council and the Natural Environment Research
471 Council, respectively.

472 References

- 473 Anthony, E.J., Brunier, G., Besset, M., Goichot, M., Dussouillez, P., Nguyen, V.L., 2015.
474 Linking rapid erosion of the Mekong River delta to human activities. *Sci. Rep.* 5, 14745.
475 <https://doi.org/10.1038/srep14745>
- 476 Bagnold, R.A., 1966. An approach to the sediment transport problem from general physics.
477 Geological Survey Professional Paper 422-I. U.S. Government Printing Office,
478 Washington, DC.
- 479 Baran, E., Myschowoda, C., 2009. Dams and fisheries in the Mekong Basin. *Aquat. Ecosyst.*
480 *Health Manag.* 12, 227–234. <https://doi.org/10.1080/14634980903149902>
- 481 Best, J., 2019. Anthropogenic stresses on the world’s big rivers. *Nat. Geosci.* 12, 7–21.
482 <https://doi.org/10.1038/s41561-018-0262-x>
- 483 Bontemps, S., Defourny, P., Bogaert, E.V., Arino, O., Kalogirou, V., Perez, J.R., 2011.
484 GLOBCOVER 2009-Products description and validation report.
- 485 Brune, G.M., 1953. Trap efficiency of reservoirs. *Trans. AGU* 34, 407–418.
- 486 Busico, G., Giuditta, E., Kazakis, N., Colombani, N., 2019. A Hybrid GIS and AHP Approach
487 for Modelling Actual and Future Forest Fire Risk Under Climate Change Accounting
488 Water Resources Attenuation Role. *Sustainability* 11, 7166.
489 <https://doi.org/10.3390/su11247166>
- 490 Bussi, G., Dadson, S.J., Prudhomme, C., Whitehead, P.G., Prudhomme, C., 2016a. Modelling
491 the future impacts of climate and land-use change on suspended sediment transport in the
492 River Thames (UK). *J. Hydrol.* 542, 357–372.
493 <https://doi.org/10.1016/j.jhydrol.2016.09.010>
- 494 Bussi, G., Janes, V., Whitehead, P.G., Dadson, S.J., Holman, I.P., 2017. Dynamic response of
495 land use and river nutrient concentration to long-term climatic changes. *Sci. Total*
496 *Environ.* 590–591, 818–831. <https://doi.org/10.1016/j.scitotenv.2017.03.069>

- 497 Bussi, G., Whitehead, P.G., Bowes, M.J., Read, D.S., Prudhomme, C., Dadson, S.J., 2016b.
498 Impacts of climate change, land-use change and phosphorus reduction on phytoplankton
499 in the River Thames (UK). *Sci. Total Environ.* 572, 1507–1519.
500 <https://doi.org/10.1016/j.scitotenv.2016.02.109>
- 501 Carling, P.A., Huang, H.Q., Su, T., Hornby, D., 2019. Flow structure in large bedrock-
502 channels: The example of macroturbulent rapids, lower Mekong River, Southeast Asia.
503 *Earth Surf. Process. Landforms* 44, 843–860. <https://doi.org/10.1002/esp.4537>
- 504 Chapman, A., Darby, S., 2016. Evaluating sustainable adaptation strategies for vulnerable
505 mega-deltas using system dynamics modelling: Rice agriculture in the Mekong Delta's
506 An Giang Province, Vietnam. *Sci. Total Environ.* 559, 326–338.
507 <https://doi.org/10.1016/j.scitotenv.2016.02.162>
- 508 Darby, S.E., Hackney, C.R., Leyland, J., Kummu, M., Lauri, H., Parsons, D.R., Best, J.L.,
509 Nicholas, A.P., Aalto, R., 2016. Fluvial sediment supply to a mega-delta reduced by
510 shifting tropical-cyclone activity. *Nature* 539, 276–279.
511 <https://doi.org/10.1038/nature19809>
- 512 Day, J.W., Agboola, J., Chen, Z., D'Elia, C., Forbes, D.L., Giosan, L., Kemp, P., Kuenzer, C.,
513 Lane, R.R., Ramachandran, R., Syvitski, J., Yañez-Arancibia, A., 2016. Approaches to
514 defining deltaic sustainability in the 21st century. *Estuar. Coast. Shelf Sci.* 183, 275–291.
515 <https://doi.org/10.1016/j.ecss.2016.06.018>
- 516 Dunn, F.E., Darby, S.E., Nicholls, R.J., Cohen, S., Zarfl, C., Fekete, B.M., 2019. Projections
517 of declining fluvial sediment delivery to major deltas worldwide in response to climate
518 change and anthropogenic stress. *Environ. Res. Lett.* 14, 084034.
519 <https://doi.org/10.1088/1748-9326/ab304e>
- 520 Edenhofer, O., Pichs-Madruga, R., Sokona, Y., Farahani, E., Kadner, S., Seyboth, K., Adler,
521 A., Baum, I., Brunner, S., Eickemeier, P., Kriemann, B., 2014. Summary for policymakers
522 climate change 2014, mitigation of climate change. IPCC 2014, Climate Change 2014:
523 Contribution of Working Group III to the Fifth Assessment Report of the
524 Intergovernmental Panel on Climate Change.
- 525 Ericson, J.P., Vorosmarty, C.J., Dingman, S.L., Ward, L.G., Meybeck, M., 2006. Effective sea-
526 level rise and deltas: Causes of change and human dimension implications. *Glob. Planet.*
527 *Change* 50, 63–82. <https://doi.org/10.1016/j.gloplacha.2005.07.004>
- 528 Farr, T.G., Rosen, P.A., Caro, E., Crippen, R., Duren, R., Hensley, S., Kobrick, M., Paller, M.,
529 Rodriguez, E., Roth, L., Seal, D., Shaffer, S., Shimada, J., Umland, J., Werner, M., Oskin,
530 M., Burbank, D., Alsdorf, D., 2007. The Shuttle Radar Topography Mission. *Rev.*
531 *Geophys.* 45, RG2004. <https://doi.org/10.1029/2005RG000183>
- 532 Futter, M.N., Erlandsson, M.A., Butterfield, D., Whitehead, P.G., Oni, S.K., Wade, A.J., 2014.
533 PERSiST: a flexible rainfall-runoff modelling toolkit for use with the INCA family of
534 models. *Hydrol. Earth Syst. Sci.* 18, 855–873. <https://doi.org/10.5194/hess-18-855-2014>

- 535 Grill, G., Lehner, B., Thieme, M., Geenen, B., Tickner, D., Antonelli, F., Babu, S., Borrelli, P.,
536 Cheng, L., Crochetiere, H., Ehalt Macedo, H., Filgueiras, R., Goichot, M., Higgins, J.,
537 Hogan, Z., Lip, B., McClain, M.E., Meng, J., Mulligan, M., Nilsson, C., Olden, J.D.,
538 Opperman, J.J., Petry, P., Reidy Liermann, C., Sáenz, L., Salinas-Rodríguez, S., Schelle,
539 P., Schmitt, R.J.P., Snider, J., Tan, F., Tockner, K., Valdujo, P.H., van Soesbergen, A.,
540 Zarfl, C., 2019. Mapping the world's free-flowing rivers. *Nature* 569, 215–221.
541 <https://doi.org/10.1038/s41586-019-1111-9>
- 542 Gupta, A., 2009. Geology and Landforms of the Mekong Basin, in: *The Mekong*. Elsevier, pp.
543 29–51. <https://doi.org/10.1016/B978-0-12-374026-7.00003-6>
- 544 Gupta, H.V., Kling, H., Yilmaz, K.K., Martinez, G.F., 2009. Decomposition of the mean
545 squared error and NSE performance criteria: Implications for improving hydrological
546 modelling. *J. Hydrol.* 377, 80–91. <https://doi.org/10.1016/j.jhydrol.2009.08.003>
- 547 Ibáñez, C., Day, J.W., Reyes, E., 2014. The response of deltas to sea-level rise: Natural
548 mechanisms and management options to adapt to high-end scenarios. *Ecol. Eng.* 65, 122–
549 130. <https://doi.org/10.1016/j.ecoleng.2013.08.002>
- 550 Janes, T., McGrath, F., Macadam, I., Jones, R., 2019. High-resolution climate projections for
551 South Asia to inform climate impacts and adaptation studies in the Ganges-Brahmaputra-
552 Meghna and Mahanadi deltas. *Sci. Total Environ.* 650, 1499–1520.
553 <https://doi.org/10.1016/j.scitotenv.2018.08.376>
- 554 Jarritt, N.P., Lawrence, D.S.L., 2006. Simulating Fine Sediment Delivery in Lowland
555 Catchments: Model Development and Application of INCA-Sed, in: Owens, P.N.,
556 Collins, A.J. (Eds.), *Soil Erosion and Sediment Redistribution in River Catchments:
557 Measurement, Modelling and Management*. CAB International, pp. 207–2016.
- 558 Kazama, S., Hagiwara, T., Ranjan, P., Sawamoto, M., 2007. Evaluation of groundwater
559 resources in wide inundation areas of the Mekong River basin. *J. Hydrol.* 340, 233–243.
560 <https://doi.org/10.1016/j.jhydrol.2007.04.017>
- 561 Kondolf, G.M., 1997. PROFILE: Hungry Water: Effects of Dams and Gravel Mining on River
562 Channels. *Environ. Manage.* 21, 533–551. <https://doi.org/10.1007/s002679900048>
- 563 Kondolf, G.M., Rubin, Z.K., Minear, J.T., 2014. Dams on the Mekong: Cumulative sediment
564 starvation. *Water Resour. Res.* 50, 5158–5169. <https://doi.org/10.1002/2013WR014651>
- 565 Kondolf, G.M., Schmitt, R.J.P., Carling, P., Darby, S.E., Arias, M., Bizzi, S., Castelletti, A.,
566 Cochrane, T.A., Gibson, S., Kummu, M., Oeurng, C., Rubin, Z., Wild, T., 2018. Changing
567 sediment budget of the Mekong: Cumulative threats and management strategies for a large
568 river basin. *Sci. Total Environ.* 625, 114–134.
569 <https://doi.org/10.1016/j.scitotenv.2017.11.361>
- 570 Kummu, M., Lu, X.X., Wang, J.J., Varis, O., 2010. Basin-wide sediment trapping efficiency
571 of emerging reservoirs along the Mekong. *Geomorphology* 119, 181–197.
572 <https://doi.org/10.1016/j.geomorph.2010.03.018>

- 573 Kummu, M., Varis, O., 2007. Sediment-related impacts due to upstream reservoir trapping, the
574 Lower Mekong River. *Geomorphology* 85, 275–293.
575 <https://doi.org/10.1016/j.geomorph.2006.03.024>
- 576 Lafon, T., Dadson, S.J., Buys, G., Prudhomme, C., 2013. Bias correction of daily precipitation
577 simulated by a regional climate model: a comparison of methods. *Int. J. Climatol.* 33,
578 1367–1381. <https://doi.org/10.1002/joc.3518>
- 579 Lázár, A.N., Butterfield, D., Futter, M.N., Rankinen, K., Thouvenot-Korppoo, M., Jarritt, N.P.,
580 Lawrence, D.S.L., Wade, A.J., Whitehead, P.G., 2010. An assessment of the fine sediment
581 dynamics in an upland river system: INCA-Sed modifications and implications for
582 fisheries. *Sci. Total Environ.* 408, 2555–2566.
583 <https://doi.org/10.1016/j.scitotenv.2010.02.030>
- 584 Li, T., Wang, S., Liu, Y., Fu, B., Zhao, W., 2018. Driving forces and their contribution to the
585 recent decrease in sediment flux to ocean of major rivers in China. *Sci. Total Environ.*
586 634, 534–541. <https://doi.org/10.1016/j.scitotenv.2018.04.007>
- 587 Lu, Q., Futter, M.N., Nizzetto, L., Bussi, G., Jürgens, M.D., Whitehead, P.G., 2016. Fate and
588 Transport of Polychlorinated Biphenyls (PCBs) in the River Thames Catchment – Insights
589 from a Coupled Multimedia Fate and Hydrobiogeochemical Transport Model. *Sci. Total*
590 *Environ.* 572, 1461–1470. <https://doi.org/10.1016/j.scitotenv.2016.03.029>
- 591 Lu, Q., Whitehead, P.G., Bussi, G., Futter, M.N., Nizzetto, L., 2017. Modelling metaldehyde
592 in catchments: a River Thames case-study. *Environ. Sci. Process. Impacts* 19, 586–595.
593 <https://doi.org/10.1039/C6EM00527F>
- 594 Lu, X., Kummu, M., Oeurng, C., 2014. Reappraisal of sediment dynamics in the Lower
595 Mekong River, Cambodia. *Earth Surf. Process. Landforms* 39, 1855–1865.
596 <https://doi.org/10.1002/esp.3573>
- 597 Lu, X.X., Siew, R.Y., 2006. Water discharge and sediment flux changes over the past decades
598 in the Lower Mekong River: possible impacts of the Chinese dams. *Hydrol. Earth Syst.*
599 *Sci.* 10, 181–195. <https://doi.org/10.5194/hess-10-181-2006>
- 600 Mekong River Commission, 2010. IWRM-based Basin Development Strategy for the Lower
601 Mekong Basin. Fourth draft. Mekong River Commission. MRC. 2010b. The Mekong
602 River Commission. (Available at: <http://www.mrcmekong.org/>. Accessed on
603 16/12/2010). United Nations Environment Programme. Afte.
- 604 Mekong River Commission, 2009. Initiative on sustainable hydropower work plan. Mekong
605 River Commission.(Available at: [http://](http://www.mrcmekong.org/programmes/hydropower/hydropower-pub.htm)
606 www.mrcmekong.org/programmes/hydropower/hydropower-pub.htm. Accessed on:
607 17/12/2010).
- 608 Meshkova, L. V., Carling, P.A., 2012. The geomorphological characteristics of the Mekong
609 River in northern Cambodia: A mixed bedrock–alluvial multi-channel network.
610 *Geomorphology* 147–148, 2–17. <https://doi.org/10.1016/j.geomorph.2011.06.041>

- 611 Milliman, J.D., Meade, R.H., 1983. World-Wide Delivery of River Sediment to the Oceans. *J.*
612 *Geol.* 91, 1–21. <https://doi.org/10.1086/628741>
- 613 Minderhoud, P.S.J., Coumou, L., Erkens, G., Middelkoop, H., Stouthamer, E., 2019. Mekong
614 delta much lower than previously assumed in sea-level rise impact assessments. *Nat.*
615 *Commun.* 10, 3847. <https://doi.org/10.1038/s41467-019-11602-1>
- 616 Nguyen, H.Q., Korbee, D., Ho, H.L., Weger, J., Thi Thanh Hoa, P., Thi Thanh Duyen, N.,
617 Dang Manh Hong Luan, P., Luu, T.T., Ho Phuong Thao, D., Thi Thu Trang, N., Hermans,
618 L., Evers, J., Wyatt, A., Chau Nguyen, X.Q., Long Phi, H., 2019. Farmer adoptability for
619 livelihood transformations in the Mekong Delta: a case in Ben Tre province. *J. Environ.*
620 *Plan. Manag.* 62, 1603–1618. <https://doi.org/10.1080/09640568.2019.1568768>
- 621 Nie, J., Ruetenik, G., Gallagher, K., Hoke, G., Garziona, C.N., Wang, W., Stockli, D., Hu, X.,
622 Wang, Z., Wang, Y., Stevens, T., Danišik, M., Liu, S., 2018. Rapid incision of the Mekong
623 River in the middle Miocene linked to monsoonal precipitation. *Nat. Geosci.* 11, 944–948.
624 <https://doi.org/10.1038/s41561-018-0244-z>
- 625 Nizzetto, L., Bussi, G., Futter, M.N., Butterfield, D., Whitehead, P.G., 2016. A theoretical
626 assessment of microplastic transport in river catchments and their retention by soils and
627 river sediments. *Environ. Sci. Process. Impacts* 18, 1050–1059.
628 <https://doi.org/10.1039/C6EM00206D>
- 629 Schmitt, R.J.P., Bizzi, S., Castelletti, A., Opperman, J.J., Kondolf, G.M., 2019. Planning dam
630 portfolios for low sediment trapping shows limits for sustainable hydropower in the
631 Mekong. *Sci. Adv.* 5, eaaw2175. <https://doi.org/10.1126/sciadv.aaw2175>
- 632 Syvitski, J.P.M., 2008. Deltas at risk. *Sustain. Sci.* 3, 23–32. [https://doi.org/10.1007/s11625-](https://doi.org/10.1007/s11625-008-0043-3)
633 [008-0043-3](https://doi.org/10.1007/s11625-008-0043-3)
- 634 Syvitski, J.P.M., Kettner, A.J., Overeem, I., Hutton, E.W.H., Hannon, M.T., Brakenridge, G.R.,
635 Day, J., Vörösmarty, C., Saito, Y., Giosan, L., Nicholls, R.J., 2009. Sinking deltas due to
636 human activities. *Nat. Geosci.* 2, 681–686. <https://doi.org/10.1038/ngeo629>
- 637 Tessler, Z.D., Vörösmarty, C.J., Grossberg, M., Gladkova, I., Aizenman, H., 2016. A global
638 empirical typology of anthropogenic drivers of environmental change in deltas. *Sustain.*
639 *Sci.* 11, 525–537. <https://doi.org/10.1007/s11625-016-0357-5>
- 640 Tessler, Z.D., Vorosmarty, C.J., Grossberg, M., Gladkova, I., Aizenman, H., Syvitski, J.P.M.,
641 Foufoula-Georgiou, E., 2015. Profiling risk and sustainability in coastal deltas of the
642 world. *Science* (80-.). 349, 638–643. <https://doi.org/10.1126/science.aab3574>
- 643 Tessler, Z.D., Vörösmarty, C.J., Overeem, I., Syvitski, J.P.M., 2018. A model of water and
644 sediment balance as determinants of relative sea level rise in contemporary and future
645 deltas. *Geomorphology* 305, 209–220. <https://doi.org/10.1016/j.geomorph.2017.09.040>
- 646 Thuc, T., Van Thang, N., Thi Lan Huong, H., Van Khiem, M., Xuan Hien, N., Ha Phong, D.,
647 2016. Climate Change and Sea Level Rise Scenarios for Viet Nam: A Summary for

648 policymakers, Report to Vietnam Ministry of Natural Resources and Environment.

649 Van, T.P.D., Carling, P.A., Atkinson, P.M., 2012. Modelling the bulk flow of a bedrock-
650 constrained, multi-channel reach of the Mekong River, Siphandone, southern Laos. *Earth*
651 *Surf. Process. Landforms* 37, 533–545. <https://doi.org/10.1002/esp.2270>

652 Vörösmarty, C.J., Meybeck, M., Fekete, B., Sharma, K., Green, P., Syvitski, J.P.M., 2003.
653 Anthropogenic sediment retention: major global impact from registered river
654 impoundments. *Glob. Planet. Change* 39, 169–190. [https://doi.org/10.1016/S0921-](https://doi.org/10.1016/S0921-8181(03)00023-7)
655 8181(03)00023-7

656 Wade, A.J., Durand, P., Beaujouan, V., Wessel, W., Raat, K.J., Whitehead, P.G., Butterfield,
657 D., Rankinen, K., Lepisto, A., 2002. A nitrogen model for European catchments: INCA,
658 new model structure and equations. *Hydrol. Earth Syst. Sci.* 6, 559–582.
659 <https://doi.org/10.5194/hess-6-559-2002>

660 Walling, D.E., 2008. The Changing Sediment Load of the Mekong River. *AMBIO A J. Hum.*
661 *Environ.* 37, 150–157. [https://doi.org/10.1579/0044-](https://doi.org/10.1579/0044-7447(2008)37[150:TCSLOT]2.0.CO;2)
662 7447(2008)37[150:TCSLOT]2.0.CO;2

663 Walling, D.E., Fang, D., 2003. Recent trends in the suspended sediment loads of the world's
664 rivers. *Glob. Planet. Change* 39, 111–126. [https://doi.org/10.1016/S0921-8181\(03\)00020-](https://doi.org/10.1016/S0921-8181(03)00020-1)
665 1

666 Wang, W., Lu, H., Ruby Leung, L., Li, H.-Y., Zhao, J., Tian, F., Yang, K., Sothea, K., 2017.
667 Dam Construction in Lancang-Mekong River Basin Could Mitigate Future Flood Risk
668 From Warming-Induced Intensified Rainfall. *Geophys. Res. Lett.* 44, 10,378-10,386.
669 <https://doi.org/10.1002/2017GL075037>

670 Whitehead, P.G., Barbour, E., Futter, M.N., Sarkar, S., Rodda, H., Caesar, J., Butterfield, D.,
671 Jin, L., Sinha, R., Nicholls, R., Salehin, M., 2015. Impacts of climate change and socio-
672 economic scenarios on flow and water quality of the Ganges, Brahmaputra and Meghna
673 (GBM) river systems: low flow and flood statistics. *Environ. Sci. Process. Impacts* 17,
674 1057–1069. <https://doi.org/10.1039/c4em00619d>

675 Whitehead, P.G., Jin, L., Bussi, G., Voepel, H.E., Darby, S.E., Vasilopoulos, G., Manley, R.,
676 Rodda, H., Hutton, C., Hackney, C., Tri, V.P.D., Hung, N.N., 2019. Water quality
677 modelling of the Mekong River basin: Climate change and socioeconomics drive flow
678 and nutrient flux changes to the Mekong Delta. *Sci. Total Environ.* 673, 218–229.
679 <https://doi.org/10.1016/j.scitotenv.2019.03.315>

680 Whitehead, P.G., Wilson, E., Butterfield, D., Seed, K., 1998. A semi-distributed integrated
681 flow and nitrogen model for multiple source assessment in catchments (INCA): Part II —
682 application to large river basins in south Wales and eastern England. *Sci. Total Environ.*
683 210–211, 559–583. [https://doi.org/10.1016/S0048-9697\(98\)00038-2](https://doi.org/10.1016/S0048-9697(98)00038-2)

684 Whitehead, P.G.G., Leckie, H., Rankinen, K., Butterfield, D., Futter, M.N.N., Bussi, G., 2016.
685 An INCA model for pathogens in rivers and catchments: Model structure, sensitivity

686 analysis and application to the River Thames catchment, UK. *Sci. Total Environ.* 572,
687 1601–1610. <https://doi.org/10.1016/j.scitotenv.2016.01.128>

688 Zarfl, C., Lumsdon, A.E., Berlekamp, J., Tydecks, L., Tockner, K., 2015. A global boom in
689 hydropower dam construction. *Aquat. Sci.* 77, 161–170. [https://doi.org/10.1007/s00027-](https://doi.org/10.1007/s00027-014-0377-0)
690 014-0377-0

691

692

1 Supplementary material

2 *Table S6. River reaches/sub-catchments and corresponding characteristics.*

INCA ID	Name	River	Sub-catchment area (km ²)	Length (m)	Stream gauge?	Lon (downstream section)	Lat (downstream section)	% arable	% grassland	% forest	% water	% urban	% bare
1	Gushui	Mekong	78476	500000	NO	98.751606	28.609973	38.51	61.19	0.01	0.04	0.00	0.25
2	Manwan	Mekong	34449	661830	NO	100.498386	24.523349	42.14	40.22	9.62	0.05	0.00	7.97
3	Ban Mau	Mekong	49004	508289	NO	101.154146	21.523381	27.92	27.42	42.83	0.87	0.14	0.82
4	Pak Beng	Mekong	49401	437269	NO	101.031725	19.850000	14.03	42.18	43.63	0.07	0.09	0.00
5	Luang Prabang	Mekong	6876	154609	NO	102.201713	20.059143	17.29	45.19	37.22	0.30	0.00	0.00
6	Luang Prabang Gauge	Mekong	27583	81276	Luang Prabang	102.130787	19.894177	4.42	61.51	33.77	0.30	0.00	0.00
7	Xayabouri	Mekong	2362	106607	NO	101.819190	19.244089	1.71	57.53	40.67	0.09	0.00	0.00
8	Pak Lay	Mekong	10109	124909	NO	101.530148	18.326022	6.51	57.25	35.62	0.62	0.00	0.00
9	Sanakham	Mekong	6876	87866	NO	101.560847	17.837641	3.64	53.58	42.49	0.29	0.00	0.00
10	Santhong-Pakchom	Mekong	7051	85882	NO	102.049941	18.199854	25.93	43.05	30.38	0.64	0.00	0.00
11	Mukdahan	Mekong	66502	766312	Mukdahan	104.743392	16.539898	50.76	21.94	26.82	0.48	0.00	0.00
12	Ban Kum	Mekong	10901	207313	NO	105.585762	15.415940	49.72	22.59	26.16	1.51	0.02	0.00
13	Latsua	Mekong	605	41526	NO	105.584129	15.329925	59.48	19.83	19.08	1.60	0.01	0.00
14	Pakse	Mekong	8111	37282	Pakse	105.800065	15.113341	49.94	23.02	24.23	2.81	0.00	0.00
15	Stung Treng	Mekong	11056	205656	NO	105.983147	13.569074	32.11	36.35	30.75	0.79	0.00	0.00
16	Stung Treng Gauge	Mekong	12911	463660	Stung Treng	105.940913	13.521594	18.78	42.08	36.06	3.08	0.00	0.00
17	Sambor-Kratie	Mekong	3437	96815	Kratie	105.949996	12.780950	8.04	41.14	49.57	1.25	0.00	0.00
18	Phnom Penh	Mekong	109790	252222	NO	104.957539	11.560835	6.55	33.71	54.93	4.81	0.00	0.00
19	River mouth	Mekong	23566	307320	NO	106.198292	9.533241	44.11	24.26	28.43	3.19	0.00	0.01
20	Nam Loi	Nam Loi	15274	351567	NO	100.722575	21.310804	77.66	10.15	8.49	3.60	0.00	0.10
21	Nam Suong	Nam Suong	5723	145064	NO	102.328473	20.051469	11.17	50.71	38.10	0.01	0.01	0.00
22	Nam Khan	Nam Khan	6942	188836	NO	102.222610	19.747571	0.03	62.05	37.92	0.00	0.00	0.00
23	Nam Ngum	Nam Ngum	8311	214685	NO	102.547535	18.529925	0.14	57.62	42.24	0.00	0.00	0.00
24	Nam Nhiep	Nam Nhiep	3757	152219	NO	103.552026	18.645862	6.94	54.14	33.65	5.27	0.00	0.00
25	Nam Cadinh	Nam Cadinh	13959	247069	NO	104.147564	18.355858	2.73	56.38	40.89	0.00	0.00	0.00
26	Se Bang Hieng	Se Bang Hieng	19959	297457	NO	105.245797	16.050037	1.02	25.94	73.00	0.04	0.00	0.00
27	Nam Mun	Nam Mun	119289	618058	NO	105.455882	15.269046	26.96	31.06	41.68	0.30	0.00	0.00
28	Se Kong	Se Kong	23385	371984	NO	106.332559	14.430805	86.06	6.06	6.74	1.11	0.03	0.00
29	Se San	Se San	15434	304239	NO	106.936557	14.039971	4.26	31.64	63.78	0.32	0.00	0.00
30	Sre Pok	Sre Pok	27212	340412	NO	107.037454	13.393443	12.24	37.69	49.42	0.65	0.00	0.00

3

4

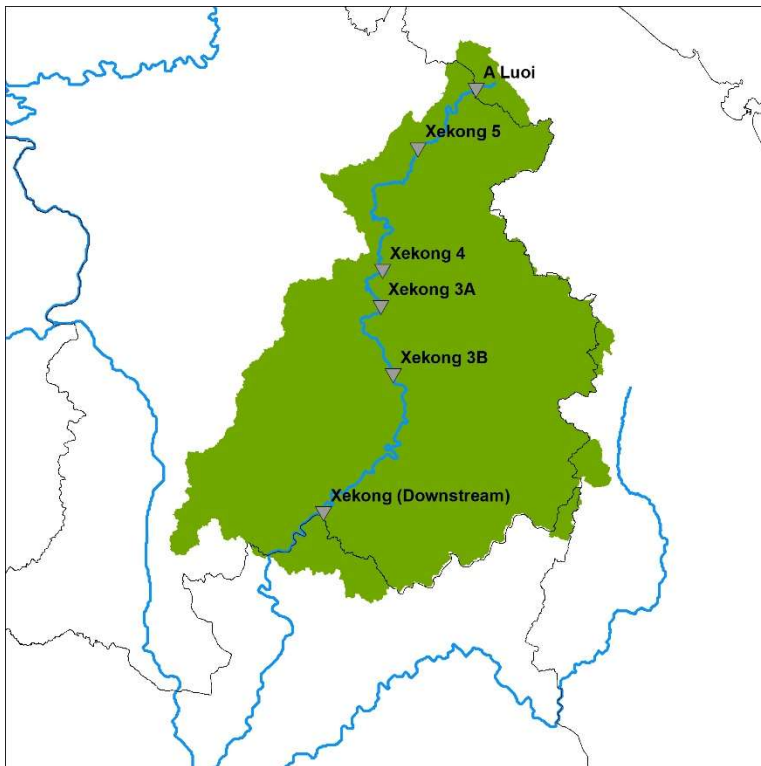
5

6 **Discussion on the aggregated reservoir trap efficiency assumption**

7 One of the assumptions of this study is that the impact of multiple reservoirs lying within a single sub-
8 catchment on the sediment transport can be approximated to the impact of a “virtual” reservoir
9 located at the sub-catchment outlet (i.e., where the most downstream dam is located), whose capacity
10 is equal to the sum of the capacity of all the dams within the sub-catchment. The main advantage of
11 this assumption is that the model structure can be kept relatively small, so to allow running a Monte
12 Carlo-like model calibration and a set of future climate projections in a reasonable amount of time.

13 While this assumption obviously carries a simplification, due to the fact that the global impact of a
14 system of dams will also depend on their corresponding locations, the characteristics of the sub-
15 catchments they drain and their sizes, we provide in this section a discussion of why this simplification
16 is reasonable for the scale and scope of the present study.

17 A simple modelling exercise was set up, using the Se Kong River as a case study. The Se Kong river is a
18 major tributary of the Mekong River. Its upper course is located almost entirely in southern Lao and
19 its confluence with the Mekong River is located near Stung Treng, in eastern Cambodia. Figure S7
20 shows the catchment extension and the river course.



21
22 *Figure S7. Se Kong River catchment and dams on its main stem.*

23 Several dams exist on its course: A Luoi, Xekong 5, Xekong 4, Xekong 3A, Xekong 3B and Xekong (total
24 reservoir capacity: 1,181 Mm³). The characteristics of the dams are shown in Figure S7.

25 *Table S7. Main characteristics of the dams on the Se Kong River.*

Dam name	Catchment area (km ²)	Storage capacity (Mm ³)	Trap efficiency (Brune, 1953)
A Luoi	399	170	96
Xekong 5	2555	330	91

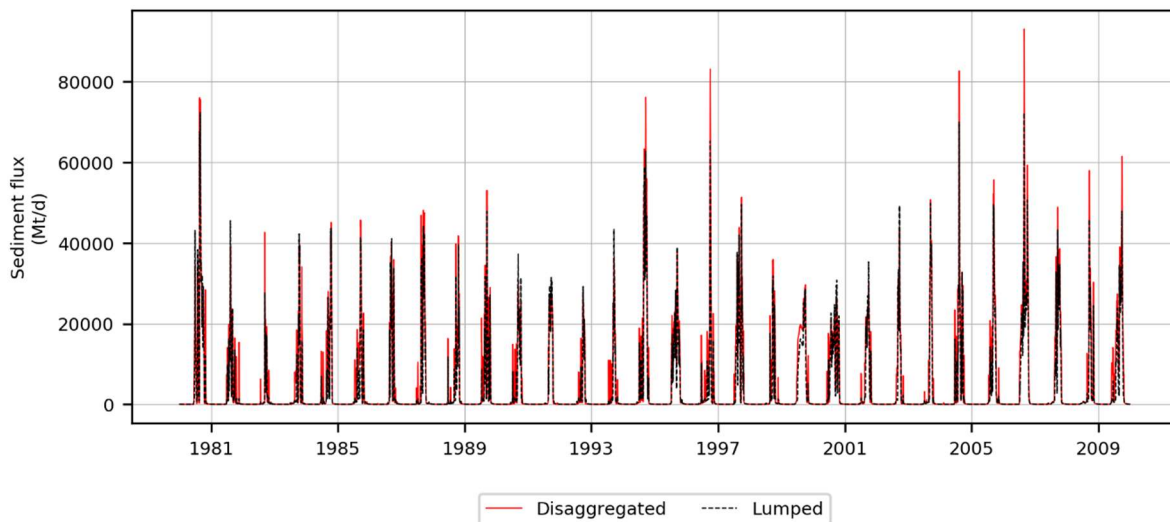
Xekong 4	5176	400	87
Xekong 3A	5883	105	64
Xekong 3B	8648	100	54
Xekong	18645	76	28

26

27 Two INCA model set-ups were implemented on the Se Kong River:

- 28 1. The catchment modelled as a single, lumped INCA catchment;
- 29 2. The catchment modelled as a set of 6 INCA sub-catchment.

30 The model parameters used in this implementation were the same parameters calibrated as shown in
 31 the paper. The effect of the dams was computed in the same way, i.e., by adjusting the sediment
 32 transport capacity to reproduce the trap efficiency computed according to Brune (1953). In the first
 33 set-up (“Lumped”), the trap efficiency of a single, “virtual” dam was computed based on the sum of
 34 the reservoir capacity of all the six reservoirs. In the second set-up (“Disaggregated”), the trap
 35 efficiency of each dam was computed based on its reservoir capacity. The model was then run for the
 36 time period 1980-2009. The model results in terms of suspended sediment flux at the catchment
 37 outlet are shown in Figure S8. It can be noticed that the two implementations obtain reasonably
 38 similar results, with only minor differences.



39

40 *Figure S8. INCA model results (daily suspended sediment flux) for the “lumped” and the “Disaggregated” model set-ups of*
 41 *the Se Kong River.*

42 This outcome shows that the error introduced by this assumption is likely to be much smaller than the
 43 other sources of modelling errors (errors in the input data, INCA model errors, climate projection
 44 errors). Furthermore, this assumption was only applied to the tributaries of the River Mekong, which
 45 account for 18% only of the total reservoir storage capacity of the Mekong catchment (being the Se
 46 Kong River storage capacity around half of all the tributary storage capacity), and therefore its
 47 potential impact is limited. While we acknowledge that a more detailed and comprehensive model
 48 could certainly be beneficial for the reduction of the errors, we believe that the relative contribution
 49 of this assumption to the global model error is reasonably low.